SPECIAL ISSUE ARTICLE

WILEY

Capacity enhancement of NOMA-SWIPT IoT relay system with direct links over rayleigh fading channels

Ashish Rauniyar[1,2] | Paal Engelstad[1,2] | Olav N. Østerbø[3]

[1]Department of Technology Systems, University of Oslo, Oslo, Norway

[2]Department of Computer Science, Oslo Metropolitan University, Oslo, Norway

[3]Telenor Research, Telenor, Oslo, Norway

Correspondence
Ashish Rauniyar, Pilestredet 52, 0167 Oslo, Norway.
Email: ashishr@ifi.uio.no

Abstract

It is known that when the direct links between the base station (BS) and the users exist and are nonnegligible, consolidating direct links could significantly enhance the performance of the cooperative relaying systems. Therefore, taking the impact of direct link into account, in this article, we investigate the capacity enhancement of the nonorthogonal multiple access (NOMA) with simultaneous wireless information and power transfer (SWIPT) for the Internet of Things (IoT) relay systems over the Rayleigh fading channels. Specifically, for the considered NOMA-SWIPT system with direct links, we study a time-switching energy harvesting (EH) architecture in which a BS transmits two symbols to the two users through the direct links and via an EH-based relay node. On the receiving user node, we employ maximum ratio combining (MRC) to show the capacity enhancement of the considered system. Moreover, analytical expressions for the Ergodic capacity and Ergodic Sum Capacity are mathematically derived for the MRC and single signal decoding scheme, and the analytical expressions are corroborated with the Monte-Carlo simulation results. This not only reveals the effect of different EH parameters on the system performance, but it also demonstrates the capacity enhancement of the considered NOMA-SWIPT system compared to a similar system without direct links and to conventional OMA schemes.

1 | INTRODUCTION

Due to the proliferation of technologies like the Internet of Things (IoT), it has been predicted that by 2025, 80 billion IoT devices will be connected to the Internet, and the global data traffic will reach up to 175 trillion gigabytes.[1] Therefore, the upcoming fifth generation (5G) and next generation networks are expected to support these massive connectivity requirements of the IoT devices.[2,3] Meeting the capacity and energy demands at the same time is a challenge that needs to be resolved.[4] The two key requirements are spectral efficiency and energy efficiency among the various challenging requirements of the 5G and the next-generation networks. Therefore, new, energy and spectral efficient protocols to ameliorate the capacity and energy demands of the massive IoT networks need to be designed. To this end, nonorthogonal multiple access (NOMA) has been contemplated as an efficient multiple access solution to support the massive connectivity of IoT and fulfill the demand of global data traffic.[5-7] Specifically, in power domain NOMA, signals of the multiple users are superposed on each other by allocating different power levels based on the perceived channel conditions. In the downlink power domain NOMA, the users with good channel conditions are allocated less power,

while the users with poor channel conditions are allocated more power.[8,9] Finally, through the process of successive interference cancellation (SIC), the users can be separated at the receiver side.[10] On the other hand, simultaneous wireless information and power transfer (SWIPT) has been considered as a promising solution to combat the issue of powering up the devices through radio frequency (RF) signals.[11-13] Thus, NOMA and SWIPT can be integrated to serve the purpose of both key requirements—spectral and energy-efficiency for the 5G and the next generation networks.[14,15] Integrating NOMA and SWIPT can also be seen as a sustainable approach for green communication in the IoT networks.

Since RF signals are abundant in nature because of the vast amount of coexisting wireless technologies, these RF signals can actually be exploited to harvest the energy.[16] This harvested energy from the RF signals can be used to power up the small IoT devices for data transmission and prolong the lifetime of such IoT networks. In this regard, through SWIPT, a device or node can harvest the energy from the RF signal and do the data transmission simultaneously.[17,18] However, considering the practical considerations of the energy harvesting (EH) circuits of the receivers, SWIPT cannot be applied directly for the information decoding (ID) at the same time. Therefore, time switching (TS) and power splitting (PS) are two popular EH architectures widely considered for SWIPT. In the TS architecture, a fraction of time is used for EH and ID separately, while in the PS architecture, the receiver splits the incoming signal into two parts by following the signal partition method for EH and ID.[19] In this article, we have used the TS architecture at the relay node because of its low complexity and ease of implementation compared to the PS architecture. However, the analysis in this article can be applied easily to other EH architectures as well.

In Reference 20, TS relaying and PS relaying protocols are proposed for the relay node to harvest the energy and ID. The authors showed that the TS relaying protocol outperformed the PS relaying protocol at relatively low signal-to-noise ratios and at high transmission rates. NOMA has been successively applied in conjugation with several technologies, such as cooperative networks and SWIPT. In Reference 21, a relay selection for the cooperative NOMA networks was studied where a two-stage relay selection strategy was proposed to achieve a minimal outage probability. In Reference 22, a best-near best-far termed as BNBF user selection scheme for NOMA-based cooperative NOMA systems with SWIPT was proposed. Here, the authors investigated the outage performance, and closed-form analytical expressions of the outage probability were derived to evaluate the system performance. Different from most of the works on cooperative NOMA with SWIPT, the work in Reference 23 proposed an RF EH and information transmission based on TS, PS, and NOMA. Here, a power-constrained IoT node operated in the dual-mode of EH and transmitted its own data along with the source node data using the NOMA protocol. The NOMA-SWIPT model was extended to include the interfering signals and further studied in Reference 24.

In cooperative communications research, a general assumption is often that a direct link to the node is not available, and the communication of data is only possible through relaying. However, in wireless communication it is known that when direct links between the base station (BS) and the users exist and are nonnegligible, consolidating direct links could significantly enhance the performance of the cooperative relaying systems.[25,26] The performance analysis of the SWIPT relaying network in the presence of a direct link was carried out in Reference 27. The authors analyzed the optimal throughput performance by considering a simple system model with a source node, a relay node, and a destination node in the presence of a direct link. A Decode-and-Forward (DF) relay was analyzed in Reference 28 for a cooperative NOMA system with direct links. Although three different relay schemes were analyzed by the authors, EH was not considered in their system model. Analyzing and studying the impact of EH in the cooperative NOMA-SWIPT systems is important for increasing the spectral and energy-efficiency demands of IoT networks. The spectral and energy efficiency of the next generation IoT networks is possible through the combined approach of NOMA with SWIPT. Thus, the authors in Reference 29 studied the outage probability of a NOMA-SWIPT network in the presence of direct links. However, the authors only studied and analyzed the outage probability for the NOMA-SWIPT network with the direct link, while the Ergodic capacity (EC) and Ergodic sum capacity (ESC) were not studied. The reason for the necessity of studying the system's EC and ESC is obvious. For the delay-tolerant transmission mode, the source transmits at any constant rate upper bounded by the EC.[30] Since the codeword length is sufficiently large compared to the block time, the codeword could experience all possible realizations of the channel. Therefore, the EC becomes an appropriate measure for the performance analysis of the system.

Motivated by the works in References 28 and 29 and taking the EC as a fundamental performance indicator, in this article, we investigate the EC performance of cooperative NOMA-SWIPT aided IoT relay systems in which one BS sends two symbols to users UE_1 and UE_2 through the direct link and via an EH-based relay node using the TS architecture. In summary, the major contributions of this article are as follows:

- Although a myriad of works have been carried out in the literature for NOMA-SWIPT systems, to the best of our knowledge, there is no published literature investigating the EC and ESC of the NOMA-SWIPT-assisted IoT relay systems with the direct link over the Rayleigh fading channels in which one BS wants to transmit two symbols to two destination nodes through the direct link and with the assistance of EH-based relay node using the TS architecture.

- Since the direct links are involved, we employ the maximum ratio combining (MRC) scheme and show the capacity enhancement of the system, by comparing it with the single signal decoding scheme (SDS).

- For the considered NOMA-SWIPT system model with direct links, we derive the analytical expressions for the EC and the ESC for both the MRC and SDS schemes and validate them by Monte-Carlo simulations, demonstrating that our derived analytical expressions are correct.

- For a fair and logical evaluation of the considered NOMA-SWIPT system with the direct link, we devised a comparable model using OMA. Along with its analytical derivations, a thorough comparison is provided between the NOMA-SWIPT and OMA-SWIPT system models without considering the impact of direct links.

- Our results demonstrate that employing the MRC scheme could significantly enhance the ESC performance of the system compared to using the SDS scheme. Moreover, we also showed that, with proper selection of EH parameters, such as the TS factor and the power allocation factor for the NOMA, the ESC performance of the system could be further improved as compared to a NOMA-SWIPT system that has no direct links and to a conventional OMA schemes.

The rest of the article is organized as follows. In Section 2, we explain the considered NOMA-SWIPT system model with the direct link scenario. Section 3, describes the system model based on TS and NOMA. In Section 4, we explain the single SDS along with its EC and ESC derivations. The MRC scheme along with its EC and ESC derivations are carried out in Section 5. EC and ESC of the OMA system model for benchmarking of results are carried out in Section 6. The performance demonstrated through the simulations is presented in Section 7. Finally, the conclusions of the article are drawn in Section 8.

2 | SYSTEM MODEL SCENARIO

The considered cooperative NOMA-SWIPT system model with direct links is shown in Figure 1. Here, a BS will transmit two symbols, x_1 and x_2, to the two destination nodes, UE_1 and UE_2, respectively, through the direct link and with the assistance of an EH-based relay node using the TS protocol. As R is a power-constrained node that acts as a DF relay, it first harvests the RF energy from the BS signal using the TS protocol, and then it decodes the symbols x_1 and x_2 transmitted by the BS in the first phase. Also, UE_1 and UE_2 receive the information transmitted by the BS through the direct links in the first phase. Then, R forwards the decoded symbols x_1 and x_2 using the NOMA protocol to the UE_1 and UE_2 in the subsequent phase. We have assumed that all nodes are considered to be operating in a half-duplex mode. Each of the communication channels faces an independent Rayleigh flat fading with additive white Gaussian noise (AWGN) with zero mean and variance σ^2. The complex channel coefficient between any two nodes is denoted by $h_i \sim CN(0, \lambda_{h_i} = d_i^{-\nu})$ where $i \in \{1, 2, 3, 4, 5\}$. $CN(0, \lambda_{h_i} = d_i^{-\nu})$ is complex normal distribution to model the Rayleigh flat fading channel with zero mean and variance λ_{h_i}, d_i is the distance between the corresponding link, and ν is the path loss exponent. The channel state information is assumed to be known at all nodes. As there exists direct links from the BS to R and UEs in our considered system model, therefore, the scenario in this article can be also depicted as the worst-case scenario of the Rician fading.

3 | SYSTEM MODEL BASED ON TS AND NOMA

In the TS relaying scheme, a power-constrained R node first harvests the energy from the BS signal for the duration of αT and then uses the time $\frac{(1-\alpha)T}{2}$ for the ID and finally $\frac{(1-\alpha)T}{2}$ for the information transmission to the UE_1 and UE_2 by following the NOMA protocol. The working of the system model based on the TS and NOMA can be explained in two phases as follows:
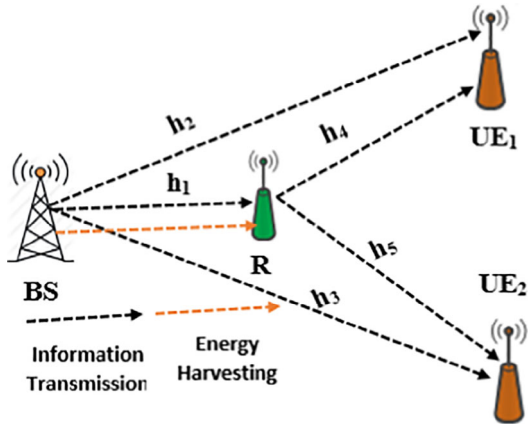
FIGURE 1 Considered System Model for the NOMA-SWIPT with Direct Links

3.1 | First phase

In the first phase, the BS broadcasts the following signal to R, UE$_1$ and UE$_2$:

$$x = \sqrt{a_1 P} x_1 + \sqrt{a_2 P} x_2 \tag{1}$$

where a_1 and a_2 are the NOMA power allocation coefficients and $a_1 > a_2$, and $a_1 + a_2 = 1$.

The received signal at R, UE$_1$ and UE$_2$ can be given, respectively, as:

$$y_R = h_1 \left(\sqrt{a_1 P} x_1 + \sqrt{a_2 P} x_2 \right) + n_R \tag{2}$$

$$y_{UE_1} = h_2 \left(\sqrt{a_1 P} x_1 + \sqrt{a_2 P} x_2 \right) + n_{UE_1} \tag{3}$$

$$y_{UE_2} = h_3 \left(\sqrt{a_1 P} x_1 + \sqrt{a_2 P} x_2 \right) + n_{UE_2} \tag{4}$$

where n_R, n_{UE_1}, and $n_{UE_2} \sim CN(0, \sigma^2 = 1)$ denote the AWGN at R, UE$_1$, and UE$_2$, respectively.

The energy harvested at R in the αT period of time is given as:

$$E_{h_{IoT_R}} = \eta P |h_1|^2 \alpha T, \tag{5}$$

where $0 \leq \eta \leq 1$ is the energy conversion efficiency. We let P_R denote the transmit power of R in the $\frac{(1-\alpha)T}{2}$ time interval. P_R is given as:

$$P_R = \frac{E_{h_{IoT_R}}}{(1-\alpha)T/2} = \frac{2\eta P |h_1|^2 \alpha}{(1-\alpha)} = k\eta P |h_1|^2 \tag{6}$$

where $k = \frac{2\alpha}{1-\alpha}$.

Now, the SINR for x_1 at R, UE$_1$ and UE$_2$ can be given, respectively, as:

$$\gamma_R^{x_1} = \frac{a_1 P |h_1|^2}{a_2 P |h_1|^2 + 1} = \frac{a_1 P X_1}{a_2 P X_1 + 1} \tag{7}$$

$$\gamma_{UE_1}^{x_1} = \frac{a_1 P |h_2|^2}{a_2 P |h_2|^2 + 1} = \frac{a_1 P X_2}{a_2 P X_2 + 1} \tag{8}$$

$$\gamma_{UE_2}^{x_1} = \frac{a_1 P |h_3|^2}{a_2 P |h_3|^2 + 1} = \frac{a_1 P X_3}{a_2 P X_3 + 1}. \tag{9}$$

Now, R and UE$_2$ decode the symbol x_2 by cancelling x_1 symbol with SIC. Therefore, the received SINR for x_2 at R and UE$_2$ can be given, respectively, as:

$$\gamma_R^{x_2} = a_2 P |h_1|^2 = a_2 P X_1 \tag{10}$$

$$\gamma_{UE_2}^{x_2} = a_2 P |h_3|^2 = a_2 P X_3. \tag{11}$$

It should be noted that in Equations (10) and (11), we have taken noise variance $\sigma^2 = 1$.

3.2 | Second phase

In this phase, R now uses the harvested energy (Equation (6)) to forward the successfully decoded symbols x_1 and x_2 to UE$_1$ and UE$_2$. R broadcasts the signal $\left(\sqrt{b_1 P_R} x_1 + \sqrt{b_2 P_R} x_2 \right)$ to UE$_1$ and UE$_2$ with b_1 and b_2 as the power allocation coefficients for the decoded symbols x_1 and x_2, respectively, and $b_1 + b_2 = 1, b_1 > b_2$.

The received signal at UE$_1$ and UE$_2$ in the second phase can be given, respectively, as:

$$y_{UE_1}^{II} = h_4 \left(\sqrt{b_1 P_R} x_1 + \sqrt{b_2 P_R} x_2 \right) + n_{UE_1}^{II} \tag{12}$$

$$y_{UE_2}^{II} = h_5 \left(\sqrt{b_1 P_R} x_1 + \sqrt{b_2 P_R} x_2 \right) + n_{UE_2}^{II} \tag{13}$$

Now, UE$_1$ decodes x_1 by treating x_2 as noise.

$$\gamma_{UE_1}^{x_1, II} = \frac{b_1 P_R |h_4|^2}{b_2 P_R |h_4|^2 + 1} = \frac{b_1 k \eta P X_1 X_4}{b_2 k \eta P X_1 X_4 + 1}. \tag{14}$$

UE$_2$ decodes x_2 after decoding x_1 and cancelling it by SIC.

$$\gamma_{UE_2}^{x_1, II} = \frac{b_1 P_R |h_5|^2}{b_2 P_R |h_5|^2 + 1} = \frac{b_1 k \eta P X_1 X_5}{b_2 k \eta P X_1 X_5 + 1} \tag{15}$$

$$\gamma_{UE_2}^{x_2, II} = b_2 P_R |h_5|^2 = b_2 P_R X_5 = b_2 k \eta P X_1 X_5. \tag{16}$$

In Equation (16), we have taken noise variance $\sigma^2 = 1$.

4 | SDS SCHEME

In the first phase of the SDS scheme, R, UE$_1$, and UE$_2$ immediately decode the symbol x_1 with the corresponding received SINR as shown in Equations (7), (8), and (9). Similarly, R, and UE$_2$ decode the symbol x_2 by cancelling the symbol x_1 with SIC. The corresponding received SINR for decoding the symbol x_2 at R, and UE$_2$ can be given by Equations (10), (11). During the second phase, UE$_1$ and UE$_2$ decode the symbols x_1 and x_2 retransmitted from the R with the received SINR as shown in Equations (14), (15), (16). Thus, during the first and second phase of the SDS scheme, a single signal or symbol 'x_1' and 'x_2' is detected at UE$_1$ and UE$_2$, respectively.

4.1 | EC and ESC Analysis for the Single SDS

By using Equations (7), (8), (9), (14) and (15), the achievable data rate of UE$_1$ associated with the symbol x_1 based on TS and NOMA for the SDS scheme is given as:

$$C_{SDS}^{x_1} = \frac{(1-\alpha)}{2} \log_2 \left(1 + \min \left(\gamma_R^{x_1}, \gamma_{UE_1}^{x_1, II}, \gamma_{UE_2}^{x_1, II}, \gamma_{UE_1}^{x_1}, \gamma_{UE_2}^{x_1} \right) \right) \tag{17}$$

Theorem 1. *The EC of* UE_1 *using TS and NOMA for the single SDS can be expressed as:*

$$
\begin{aligned}
C^{x_1}_{\text{SDS-Ana}} = \frac{(1-\alpha)}{2\ln 2} \int_{\gamma=0}^{\frac{a_1}{a_2}} \frac{\lambda_{h_1}}{1+\gamma} e^{-\frac{(\lambda_{h_2}+\lambda_{h_3})\gamma}{P(a_1-\gamma a_2)}} \Bigg(& 2\sqrt{\frac{(\lambda_{h_4}+\lambda_{h_5})\gamma}{k\eta P\lambda_{h_1}(b_1-\gamma b_2)}} K_1\left(2\sqrt{\frac{(\lambda_{h_4}+\lambda_{h_5})\gamma \lambda_{h_1}}{k\eta P(b_1-\gamma b_2)}}\right) \\
& - \sum_{n=0}^{\infty} \frac{(-1)^n}{n!}\lambda_{h_1}^n \left(\frac{\gamma}{P(a_1-\gamma a_2)}\right)^{n+1} E_{n+2}\left(\frac{(\lambda_{h_4}+\lambda_{h_5})(a_1-\gamma a_2)}{k\eta(b_1-\gamma b_2)}\right) \Bigg) d\gamma
\end{aligned}
\tag{18}
$$

■

Proof. The proof is given in Appendix A1.

Corollary 1. *In Theorem 1, when* $\lambda_{h_2}=0$ *and* $\lambda_{h_3}=0$, *the analytical expression for EC of* UE_1 *using TS and NOMA without direct links (WDLs) can be expressed as:*

$$
\begin{aligned}
C^{x_1}_{\text{WDL-Ana}} = \frac{(1-\alpha)}{2\ln 2} \int_{\gamma=0}^{\frac{a_1}{a_2}} \frac{\lambda_{h_1}}{1+\gamma} \Bigg(& 2\sqrt{\frac{(\lambda_{h_4}+\lambda_{h_5})\gamma}{k\eta P\lambda_{h_1}(b_1-\gamma b_2)}} K_1\left(2\sqrt{\frac{(\lambda_{h_4}+\lambda_{h_5})\gamma \lambda_{h_1}}{k\eta P(b_1-\gamma b_2)}}\right) \\
& - \sum_{n=0}^{\infty} \frac{(-1)^n}{n!}\lambda_{h_1}^n \left(\frac{\gamma}{P(a_1-\gamma a_2)}\right)^{n+1} E_{n+2}\left(\frac{(\lambda_{h_4}+\lambda_{h_5})(a_1-\gamma a_2)}{k\eta(b_1-\gamma b_2)}\right) \Bigg) d\gamma
\end{aligned}
\tag{19}
$$

■

Proof. Substituting $\lambda_{h_2}=0$ and $\lambda_{h_3}=0$, the proof can be derived by following the same steps as in Theorem 1. ■

Now, by using Equations (10), (11), and (16), the achievable data rate of UE_2 associated with the symbol x_2 based on TS and NOMA for the SDS scheme is given as:

$$
C^{x_2}_{\text{SDS}} = \frac{1}{2}\log_2\left(1+\min\left(\gamma_R^{x_2}, \gamma_{UE_2}^{x_2,II}, \gamma_{UE_2}^{x_2}\right)\right)
\tag{20}
$$

Theorem 2. *The EC of* UE_2 *using TS and NOMA for the single SDS can be expressed as:*

$$
C^{x_2}_{\text{SDS-Ana}} = \frac{(1-\alpha)}{2\ln 2} \int_{\gamma=0}^{\infty} \frac{\lambda_{h_1}}{1+\gamma} e^{-\frac{\lambda_{h_3}\gamma}{a_2 P}} \Bigg(2\sqrt{\frac{\lambda_{h_5}\gamma}{b_2 k\eta P\lambda_{h_1}}} K_1\left(2\sqrt{\frac{\lambda_{h_1}\lambda_{h_5}\gamma}{b_2 k\eta P}}\right) - \sum_{n=0}^{\infty} \frac{(-1)^n}{n!}\lambda_{h_1}^n \left(\frac{\gamma}{a_2 P}\right)^{n+1} E_{n+2}\left(\frac{\lambda_{h_5}a_2}{b_2 k\eta}\right) \Bigg) d\gamma
\tag{21}
$$

Proof. The proof is given in Appendix B1. ■

Corollary 2. *In Theorem 2, when* $\lambda_{h_2}=0$ *and* $\lambda_{h_3}=0$, *the analytical expression for EC of* UE_2 *using TS and NOMA WDL can be expressed as:*

$$
C^{x_2}_{\text{WDL-Ana}} = \frac{(1-\alpha)}{2\ln 2} \int_{\gamma=0}^{\infty} \frac{\lambda_{h_1}}{1+\gamma} \Bigg(2\sqrt{\frac{\lambda_{h_5}\gamma}{b_2 k\eta P\lambda_{h_1}}} K_1\left(2\sqrt{\frac{\lambda_{h_1}\lambda_{h_5}\gamma}{b_2 k\eta P}}\right) - \sum_{n=0}^{\infty} \frac{(-1)^n}{n!}\lambda_{h_1}^n \left(\frac{\gamma}{a_2 P}\right)^{n+1} E_{n+2}\left(\frac{\lambda_{h_5}a_2}{b_2 k\eta}\right) \Bigg) d\gamma
\tag{22}
$$

Proof. Substituting $\lambda_{h_2}=0$ and $\lambda_{h_3}=0$, the proof can be derived by following the same steps as in Theorem 2. ■

Now, by combining Equations (18) and (20), the analytical expression for the ESC of the considered system based on TS and NOMA with direct links for the SDS scheme is given by:

$$
C^{\text{SDS}}_{\text{ESum}} = C^{x_1}_{\text{SDS-Ana}} + C^{x_2}_{\text{SDS-Ana}}
\tag{23}
$$

Similarly, by combining Equations (19) and (22), the analytical expression for the ESC of the considered system based on TS and NOMA WDL is given by:

$$
C^{\text{WDL}}_{\text{ESum}} = C^{x_1}_{\text{WDL-Ana}} + C^{x_2}_{\text{WDL-Ana}}
\tag{24}
$$

It should be noted that the final analytical expression of $C^{x_1}_{\text{SDS-Ana}}$, $C^{x_2}_{\text{SDS-Ana}}$, $C^{x_1}_{\text{WDL-Ana}}$ and $C^{x_1}_{\text{WDL-Ana}}$ as shown in Theorem 1, Theorem 2, Corollary 1 and Corollary 2, respectively, contain an integral term which is difficult to

evaluate in closed form, but it can be evaluated through numerical approaches using software such as MATLAB or Mathematica.

5 | MRC DECODING SCHEME

As the achievable data rate is limited by the inferior channel, in the MRC scheme, UE_1 and UE_2 will not decode the received signal in the first phase. UE_1 and UE_2 will instead conserve the signal and jointly decode the signal through the MRC scheme after receiving the decoded symbol x_1 and x_2 from R in the second phase. Therefore, the corresponding SINR during the second stage for x_1 and x_2 through the MRC scheme at UE_1 and UE_2 can be, respectively, given as:

$$\gamma_{\text{MRC}}^{x_1} = \frac{a_1 P X_2}{a_2 P X_2 + 1} + \frac{b_1 k \eta P X_1 X_4}{b_2 k \eta P X_1 X_4 + 1} \tag{25}$$

$$\gamma_{\text{MRC}}^{x_2} = a_2 P X_3 + b_2 k \eta P X_1 X_5 \tag{26}$$

5.1 | EC and ESC Analysis for the MRC Decoding Scheme

By using the Equations (7), (9), (15), and (26), the achievable data rate of UE_1 associated with the symbol x_1 based on TS and NOMA for the MRC scheme can be given as:

$$C_{MRC}^{x_1} = \frac{(1-\alpha)}{2} \log_2 \left(1 + \min \left(\gamma_R^{x_1}, \gamma_{UE_2}^{x_1}, \gamma_{UE_2}^{x_1,II}, \gamma_{MRC}^{x_1} \right) \right) \tag{27}$$

Theorem 3. *The EC of* UE_1 *using TS and NOMA for the MRC decoding scheme can be expressed as:*

$$C_{\text{MRC-Ana}}^{x_1} = \frac{(1-\alpha)}{2 \ln 2} \int_{\gamma=0}^{\frac{a_1}{a_2}} \frac{1}{1+\gamma} \left(e^{-\frac{\lambda_{h_3}\gamma}{P(a_1-\gamma a_2)}} \int_{x_1=\frac{\gamma}{P(a_1-\gamma a_2)}}^{\infty} e^{-\frac{\lambda_{h_5}\gamma}{k\eta P(b_1-b_2\gamma)x_1}} \right.$$

$$\left. \times \left(\int_{z=c_3}^{\hat{z}} \frac{\lambda_{h_2}}{c_4} e^{-\frac{c_1}{c_4}} e^{\frac{\lambda_{h_2}c_3}{c_4}} e^{-\frac{(c_2 c_4 - c_1 c_3)}{c_4 z} - \frac{\lambda_{h_2}z}{c_4}} dz + e^{-\frac{\lambda_{h_2}\gamma}{(a_1-a_2\gamma)P}} \right) \lambda_{h_1} e^{-\lambda_{h_1}x_1} dx_1 \right) d\gamma \tag{28}$$

where $c_1 = \lambda_{h_4} P(a_2\gamma - a_1), c_2 = \lambda_{h_4}\gamma, c_3 = k\eta P x_1(b_1 - \gamma b_2), c_4 = k\eta P^2 x_1(b_1 a_2 - b_2(a_2\gamma - a_1)), \hat{z} = c_3 + c_4 \frac{\gamma}{(a_1-a_2\gamma)P}$

Proof. The proof is given in Appendix C1. ∎

Now, by using Equations (10) and (25), the achievable data rate of UE_2 associated with the symbol x_2 based on TS and NOMA for the MRC scheme can be given as:

$$C_{\text{MRC}}^{x_2} = \frac{(1-\alpha)}{2} \log_2 \left(1 + \min \left(\gamma_R^{x_2}, \gamma_{MRC}^{x_2} \right) \right) \tag{29}$$

Theorem 4. *The EC of* UE_2 *using TS and NOMA for the MRC decoding scheme can be expressed as:*

$$C_{\text{MRS-Ana}}^{x_2} = \frac{(1-\alpha)}{2 \ln 2} \int_{\gamma=0}^{\infty} \frac{1}{1+\gamma} \left(\int_{x_1=\frac{\gamma}{a_2 P}}^{\infty} \lambda_{h_1} \lambda_{h_3} \frac{b_2 k \eta x_1}{b_2 k \eta \lambda_{h_3} x_1 - a_2 \lambda_{h_5}} e^{-\frac{\lambda_{h_5}\gamma}{b_2 k \eta P x_1} - \lambda_{h_1}x_1} dx_1 \right.$$

$$\left. - \int_{x_1=\frac{\gamma}{a_2 P}}^{\infty} \lambda_{h_3} \frac{b_2 k \eta x_1}{b_2 k \eta \lambda_{h_3} x_1 - a_2 \lambda_{h_5}} e^{-\frac{\lambda_{h_5}\gamma}{b_2 k \eta P x_1}} e^{-\frac{(b_2 k \eta \lambda_{h_3} x_1 - a_2 \lambda_{h_5})\gamma}{b_2 k \eta P x_1 a_2 P}} \lambda_{h_1} e^{-\lambda_{h_1}x_1} dx_1 + e^{-\frac{(\lambda_{h_1}+\lambda_{h_3})\gamma}{a_2 P}} \right) d\gamma \tag{30}$$

Proof. The proof is given in Appendix D1. ∎

Now, by combining the Equations (28) and Equation (30), we get the analytical expression for the ESC of the considered system based on TS and NOMA with direct links for the MRC scheme.

It should again be noted that the final analytical expression of $C^{x_1}_{MRC-Ana}$, and $C^{x_2}_{MRC-Ana}$ as shown in Theorem 3, and Theorem 4, respectively, contain an integral term which is difficult to evaluate in closed form, but it can be evaluated through numerical approaches using software such as MATLAB or Mathematica.

6 | EC AND ESC OF OMA - FOR BENCHMARKING OF RESULTS

To evaluate the performance and demonstrate the capacity enhancement of our NOMA-SWIPT IoT relay system with a direct link, an OMA scheme using time-division multiple access (TDMA) referred to as OMA-TDMA, is considered. In the OMA-TDMA scheme, the time slots, each of the duration T, can be arranged into four time slots. In the first time slot, the BS broadcasts the signal x_1 to R and UE_1. Since R is an EH based relay, it first harvests the energy from the BS's signal for a period of αT and then uses the time $(1 - \alpha)T$ for ID. In the second time slot, R now broadcasts the decoded symbol X_1 to UE_1. Similarly, the process is repeated for the symbol x_2 for the UE_2 through the direct link and via an EH based relay R in the next two time slots. For a fair comparison with our NOMA-SWIPT system model with direct links, similar to our discussion on the SDS and MRC scheme in the above section, the user nodes UE_1 and UE_2 in the OMA-TDMA scheme can also apply the SDS or MRC scheme. Also, it should be noted that in our model, the power of the BS and the EH based R node is divided by allocating the power allocation coefficients a_1, a_2, b_1 and b_2 and thus allowing BS and R to transmit x_1 and x_2 symbols with full power. OMA-TDMA scheme would not represent a fair and reasonable comparison with our NOMA-SWIPT model. Instead, we resort to allocating the same power allocation coefficients, b_1 and b_2 at the R in both the NOMA-SWIPT system model and the OMA-TDMA scheme.

In the OMA-TDMA scheme, the transmit power of the EH based DF relay node R is given by:

$$P_{R-OT} = \frac{\eta \alpha P |h_1|^2}{1 - \alpha} \tag{31}$$

The EC of UE_1 for OMA-TDMA that is using the SDS scheme and the MRC scheme is given respectively by:

$$C^{x_1}_{\text{OMA-SDS}} = \frac{(1 - \alpha)}{4} \log_2(1 + \min(P|h_2|^2, P|h_1|^2, b_1 P_{R-OT} |h_4|^2)) \tag{32}$$

$$C^{x_1}_{\text{OMA-MRC}} = \frac{(1 - \alpha)}{4} \log_2(1 + \min(P|h_1|^2, P|h_2|^2 + b_1 P_{R-OT} |h_4|^2)) \tag{33}$$

Similarly, the EC of UE_2 for OMA-TDMA that is using the SDS scheme and the MRC scheme is given respectively by:

$$C^{x_2}_{\text{OMA-SDS}} = \frac{(1 - \alpha)}{4} \log_2(1 + \min(P|h_3|^2, P|h_1|^2, b_2 P_{R-OT} |h_5|^2)) \tag{34}$$

$$C^{x_2}_{\text{OMA-MRC}} = \frac{(1 - \alpha)}{4} \log_2(1 + \min(P|h_1|^2, P|h_3|^2 + b_2 P_{R-OT} |h_5|^2)) \tag{35}$$

Now, by combining Equations (32) and (34), we get the ESC of the OMA-TDMA model that is using the SDS scheme. Similarly, by combining Equations (33) and (35), we get the ESC of the OMA-TDMA model that is using the MRC scheme.

7 | NUMERICAL RESULTS AND DISCUSSIONS

In this section, we use Monte-Carlo simulations to test the correctness of our derived mathematical expressions for the EC and ESC of the system and make performance comparisons with the system model WDL and with the conventional OMA scheme. Unless otherwise stated, the simulation parameters used in the experiments are specified in Table 1. We used MATLAB for the Monte-Carlo experiments by averaging over 10^5 random realization of Rayleigh fading channels, i.e. h_1, h_2, h_3, h_4 and h_5. In all the results presented in this section, the legends in the figures 'SDS Ana' and 'SDS Sim' represent the analytical and simulation results for the NOMA-SWIPT model with direct links that is using the single signal detection scheme. Similarly, 'MRC Ana' and 'MRC Sim' represent the analytical and simulation results for the NOMA-SWIPT model with direct links that is using the MRC detection scheme. 'WDL

T A B L E 1 Simulation parameters

Parameter	Symbol	Values
Distance between BS and R	d_1	2.0 m
Distance between BS and UE$_1$	d_2	3.0 m
Distance between BS and UE$_2$	d_3	1.5 m
Distance between R and UE$_1$	d_4	2.0 m
Distance between R and UE$_2$	d_5	1.0 m
Path loss exponent	v	3
BS transmit SNR	δ	0-45 dB
Energy harvesting efficiency	η	0.9
Power allocation factor for NOMA	a_1	0.8
Power allocation factor for NOMA	a_2	0.2
Power allocation factor for NOMA	b_1	0.8
Power allocation factor for NOMA	b_2	0.2

Abbreviation: SNR, Signal-to-noise ratio.

F I G U R E 2 Ergodic Capacity of UE$_1$
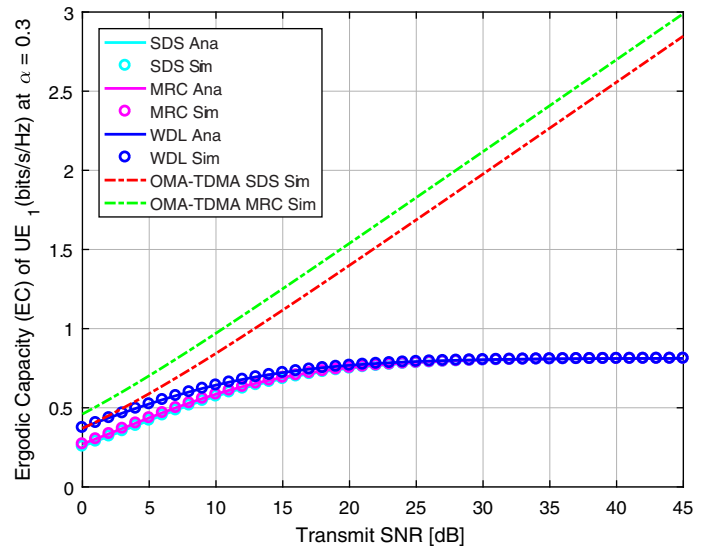
Ana' and 'WDL Sim' represent the analytical and simulation results of the NOMA-SWIPT system that is not using direct links, that is, without direct links stands for 'WDLs'. 'OMA-TDMA SDS Sim' and 'OMA-TDMA MRC Sim' represent the Monte-Carlo simulation results for the single signal detection and MRC scheme for the OMA-TDMA system model.

In Figures 2 and 3, we plot the ECs of UE$_1$ and UE$_2$ with the TS factor $\alpha = 0.3$ against the transmit SNR. As UE$_1$ is a distant user with poor channel conditions compared to UE$_2$, we observe that the EC of UE$_1$ is worse than that of UE$_2$. The ECs of UE$_1$ of the OMA-TDMA schemes that are using the SDS or MRC schemes are higher than our NOMA-SWIPT model with direct links. However, the EC for the NOMA-SWIPT model with direct links is superior to the OMA-TDMA scheme, as shown in Figure 3. As expected, the MRC scheme outperforms the SDS scheme. Also, one could argue this is not the case in Figure 2. Moreover, OMA-TDMA gives a more equal and fair sharing of capacity between UE$_1$ and UE$_2$.

In Figure 4, we plot the ESC at $\alpha = 0.3$ and $\alpha = 0.7$ against the transmit Signal-to-noise ratio (SNR) for all the schemes for a thorough comparison. We observe that the ESC is an increasing function with respect to increase in the transmit SNR for all of the schemes. At low transmit SNR, i.e. less than 10 dB, the OMA-TDMA MRC scheme has higher ESC than our NOMA-SWIPT model with direct links. However, as we increase the transmit SNR, the ESC of our NOMA-SWIPT model gives the overall higher ESC for the system. The reason for OMA-TDMA MRC scheme to have better ESC at low transmit
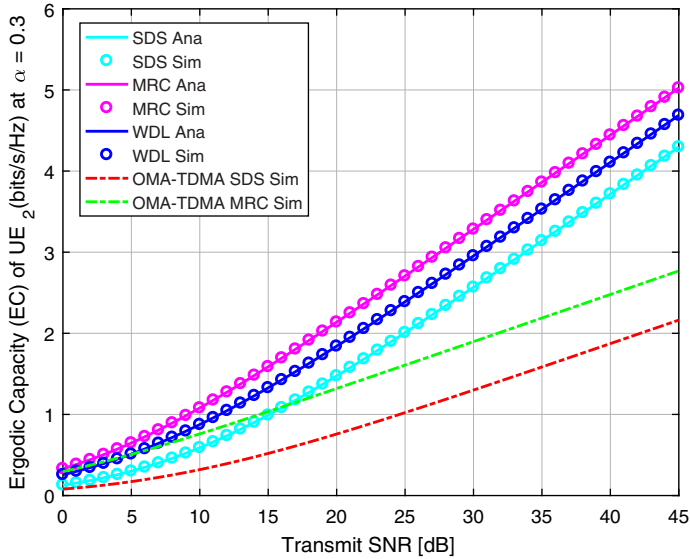
FIGURE 3 Ergodic capacity of UE$_2$
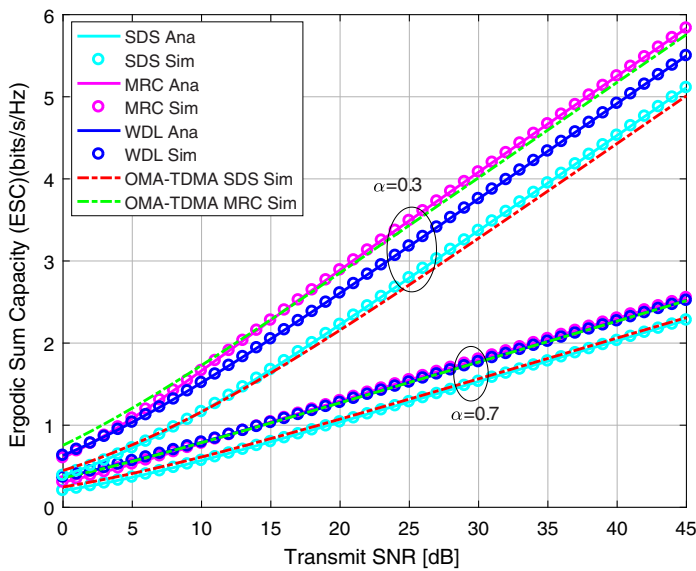
FIGURE 4 Ergodic sum capacity of considered system model for the NOMA-SWIPT with the direct link

SNR is that the BS transmits the signal for UE$_1$ and UE$_2$ with its full power of BS in two time slots whereas, in our considered NOMA-SWIPT model, the power of the BS is divided into two parts for the UE$_1$ and UE$_2$ using a single time slot. Also, it is interesting to note that the NOMA-SWIPT model WDLs has higher EC for UE$_2$ than our considered NOMA-SWIPT model with direct links that is using the SDS scheme. The reason for this is that the EC is dominated by the weakest link. Moreover, as we increase the α factor from 0.3 to 0.7, we see that the ESCs for all the models decrease. This indicates that a small α factor is sufficient for the system to harvest enough energy and the remaining time can be used for the data transmission.

In order to investigate the impact of α factor on the ESC performance, we plot the ESC against various α at the transmit SNR 25 dB and 10 dB in Figure 5. We observe that the ESC for all of the considered system models except the OMA-TDMA MRC scheme increases with an increase in α factor, until it reaches up to a maximum, and then it decreases again. This confirms that the ESC is a concave function that has a unique maxima at which the ESC of the system is maximized. The optimal α factor can be easily found, e.g., using the Golden section search method as in.[23] Also, as expected, a higher transmit SNR increases the ESC, as observed in Figure 5.

Since, the power allocation factor plays an important role in the NOMA-SWIPT system, in Figure 6, we plot the ESC against the power allocation coefficient factor b_1. When plotting the results in Figure 6, all other factors, such as $b_2 = 0.2$, $a_1 = 0.8$, and $a_2 = 0.2$ remained fixed and $\alpha = 0.3$. The reason for choosing to plot the ESC against the power allocation

FIGURE 5 Ergodic sum capacity vs time switching factor
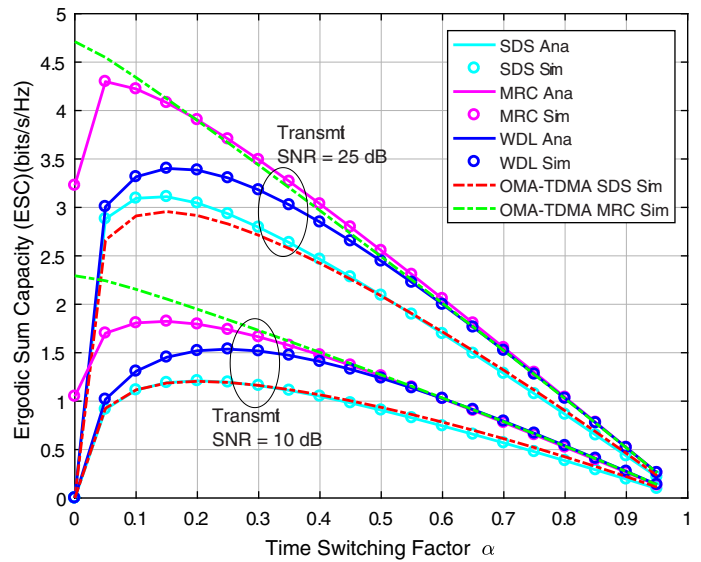
FIGURE 6 Ergodic sum capacity vs power allocation coefficient b_1
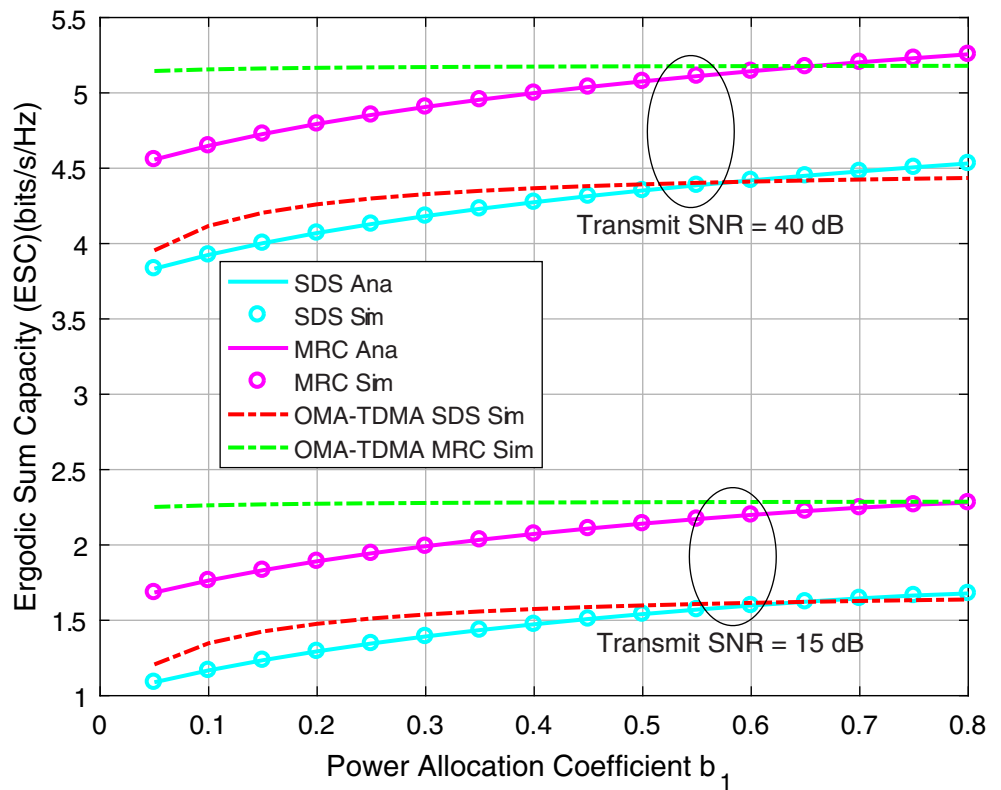
coefficient factor b_1 is that b_1 is the power allocated to the weak channel user UE_1, and b_1 factor determines the highest power allocation factor from the harvested energy at R that it is used for the data transmission to UE_1. We observe that the OMA-TDMA scheme outperforms our NOMA-SWIPT model with direct links when the power allocation coefficient factor b_1 is less than 0.6. When the value of b_1 increases beyond 0.6, the ESC of our NOMA-SWIPT model increases for both the SDS and MRC schemes. This confirms that the value of the power allocation coefficient factor needs to be selected carefully to achieve the best ESC performance.

Next, we intend to verify the ESC performance of our system model with the same power allocation coefficients of a_1 and a_2 for the OMA-TDMA system, to see the effect of ESC on the system. It should be noted that for the OMA-TDMA system, we assumed that the BS transmits the signals to UE_1 and UE_2 with the full power. However, for our NOMA-SWIPT model, the BS power is divided for the data transmission of the UE_1 and UE_2 by the power allocation coefficients a_1
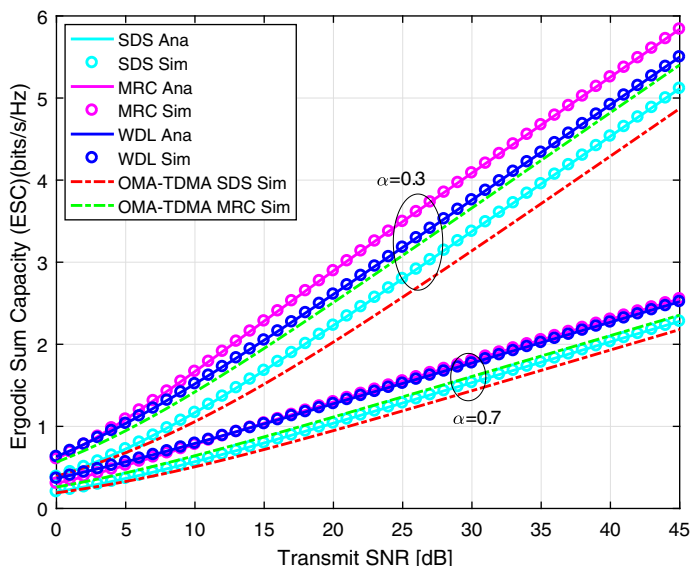
and a_2. Therefore, in Figure 7, we see that, if we allocate the same power allocation coefficients of a_1 and a_2 for the OMA-TDMA system for a fair comparison with our NOMA-SWIPT model with direct links, the ESC performance of our model outperforms the OMA-TDMA system model for both the MRC and SDS schemes. Also, it is observed that the ESC of the NOMA-SWIPT system model that is not using direct links outperformed the ESC performance of the OMA-TDMA system for both the SDS and MRC scheme. This indicates the performance gain in the ESC of the NOMA-SWIPT system over the OMA-TDMA SWIPT system.

8 | CONCLUSION

It is understood that consolidating direct links can significantly improve the efficiency of cooperative relaying systems when there are direct links between the BS and the users. Therefore, in this article, we investigated how direct links improve the capacity of the NOMA-SWIPT IoT relay systems with Rayleigh fading channels. Specifically, by employing the MRC scheme, we showed how direct links enhance the capacity of our NOMA-SWIPT system model with a TS EH architecture. For a detailed study and a fair comparison of the NOMA-SWIPT system model with direct links, we also studied the model without considering direct links and also other OMA-TDMA SWIPT models. The analytical expressions for the NOMA-SWIPT model with and WDLs for both MRC and SDS schemes were mathematically derived and analyzed and finally corroborated with the Monte-Carlo simulation results. Our results demonstrated that the MRC scheme can significantly enhance the ESC performance of the system compared to the SDS scheme. Moreover, we also showed that, with a proper selection of EH parameters, such as TS factor and power allocation factor for the NOMA, the ESC performance of the system can be further improved compared to the NOMA-SWIPT system that is not using direct links and compared to conventional OMA schemes.

ORCID

Ashish Rauniyar https://orcid.org/0000-0002-2142-9522

REFERENCES

1. Reinsel D, Gantz J, Rydning J. Data age 2025: the digitization of the world from edge to core. *Seagate*. 2018; Doc# US44413318:1-28. https://www.seagate.com/files/www-content/our-story/trends/files/idc-seagate-dataage-whitepaper.pdf.
2. Bockelmann C, Pratas NK, Wunder G, et al. Towards massive connectivity support for scalable mMTC communications in 5G networks. *IEEE Access*. 2018;6:28969-28992.
3. Al-Falahy N, Alani OY. Technologies for 5G networks: challenges and opportunities. *IT Professional*. 2017;19(1):12-20.
4. Singh S, Saxena N, Roy A, Kim H. Energy efficiency in wireless networks–a composite review. *IETE Tech Rev*. 2015;32(2):84-93.
5. Ali KS, Haenggi M, ElSawy H, Chaaban A, Alouini MS. Downlink non-orthogonal multiple access (NOMA) in poisson networks. *IEEE Trans Commun*. 2018;67(2):1613-1628.

6. Basharat M, Ejaz W, Naeem M, Khattak AM, Anpalagan A. A survey and taxonomy on nonorthogonal multiple-access schemes for 5G networks. *Trans Emerg Telecommun Technol*. 2018;29(1):e3202.

7. Wan D, Wen M, Ji F, Yu H, Chen F. Non-orthogonal multiple access for cooperative communications: challenges, opportunities, and trends. *IEEE Wirel Commun*. 2018;25(2):109-117.

8. Islam SR, Avazov N, Dobre OA, Kwak KS. Power-domain non-orthogonal multiple access (NOMA) in 5G systems: potentials and challenges. *IEEE Commun Surv Tutor*. 2016;19(2):721-742.

9. Zhang Y, Yang Z, Feng Y, Yan S. Performance analysis of cooperative relaying systems with power-domain non-orthogonal multiple access. *IEEE Access*. 2018;6:39839-39848.

10. Chen X, Jia R, Ng DWK. On the design of massive non-orthogonal multiple access with imperfect successive interference cancellation. *IEEE Trans Commun*. 2018;67(3):2539-2551.

11. Zhai D, Zhang R, Du J, Ding Z, Yu FR. Simultaneous wireless information and power transfer at 5G new frequencies: channel measurement and network design. *IEEE J Select Areas Commun*. 2018;37(1):171-186.

12. Liu X, Zhang X, Jia M, Fan L, Lu W, Zhai X. 5G-based green broadband communication system design with simultaneous wireless information and power transfer. *Phys Commun*. 2018;28:130-137.

13. Chae SH, Jeong C, Lim SH. Simultaneous wireless information and power transfer for internet of things sensor networks. *IEEE Internet Things J*. 2018;5(4):2829-2843.

14. Kader MF, Uddin MB, Islam A, Shin SY. Cooperative non-orthogonal multiple access with SWIPT over Nakagami-m fading channels. *Trans Emerg Telecommun Technol*. 2019;30(5):e3571.

15. Zaidi SK, Hasan SF, Gui X. SWIPT-aided uplink in hybrid non-orthogonal multiple access. Paper presented at: Proceedings of the IEEE Wireless Communications and Networking Conference (WCNC); 2018:1-6; IEEE.

16. Huang S, Yao Y, Feng Z. Simultaneous wireless information and power transfer for relay assisted energy harvesting network. *Wirel Netw*. 2018;24(2):453-462.

17. Aboelwafa MM, Abd-Elmagid MA, Biason A, Seddik KG, ElBatt T, Zorzi M. Towards optimal resource allocation in wireless powered communication networks with non-orthogonal multiple access. *Ad Hoc Netw*. 2019;85:1-10.

18. Huang J, Xing CC, Wang C. Simultaneous wireless information and power transfer: technologies, applications, and research challenges. *IEEE Commun Mag*. 2017;55(11):26-32.

19. Gu Y, Aissa S. RF-based energy harvesting in decode-and-forward relaying systems: ergodic and outage capacities. *IEEE Trans Wirel Commun*. 2015;14(11):6425-6434.

20. Nasir AA, Zhou X, Durrani S, Kennedy RA. Relaying protocols for wireless energy harvesting and information processing. *IEEE Trans Wirel Commun*. 2013;12(7):3622-3636.

21. Ding Z, Dai H, Poor HV. Relay selection for cooperative NOMA. *IEEE Wirel Commun Lett*. 2016;5(4):416-419.

22. Do NT, Da Costa DB, Duong TQ, An B. A BNBF user selection scheme for NOMA-based cooperative relaying systems with SWIPT. *IEEE Commun Lett*. 2016;21(3):664-667.

23. Rauniyar A, Engelstad P, Østerbø O. RF energy harvesting and information transmission based on NOMA for wireless powered IoT relay systems. *Sensors*. 2018;18(10):3254.

24. Rauniyar A, Engelstad PE, Østerbø ON. Performance analysis of RF energy harvesting and information transmission based on NOMA with interfering signal for IoT relay systems. *IEEE Sensors J*. 2019;19(17):7668-7682. https://doi.org/10.1109/JSEN.2019.2914796.

25. Kim JB, Lee IH. Non-orthogonal multiple access in coordinated direct and relay transmission. *IEEE Commun Lett*. 2015;19(11):2037-2040.

26. Kim JB, Lee IH, Lee J. Capacity scaling for D2D aided cooperative relaying systems using NOMA. *IEEE Wirel Commun Lett*. 2017;7(1):42-45.

27. Zhao N, Hu F, Li Z, Gao Y. Simultaneous wireless information and power transfer strategies in relaying network with direct link to maximize throughput. *IEEE Trans Veh Technol*. 2018;67(9):8514-8524.

28. Liu H, Ding Z, Kim KJ, Kwak KS, Poor HV. Decode-and-forward relaying for cooperative NOMA systems with direct links. *IEEE Trans Wirel Commun*. 2018;17(12):8077-8093.

29. Ha DB, Nguyen SQ. Outage performance of energy harvesting DF relaying NOMA networks. *Mobile Netw Appl*. 2018;23(6):1572-1585.

30. Zhong C, Suraweera HA, Zheng G, Krikidis I, Zhang Z. Improving the throughput of wireless powered dual-hop systems with full duplex relaying. Paper presented at: Proceedings of the IEEE International Conference on Communications (ICC); 2015:4253-4258; IEEE.

31. Gradshteyn IS, Ryzhik IM. *Table of Integrals, Series, and Products*. Cambridge, MA: Academic Press; 1980.

APPENDIX A

Proof of Theorem 1. The cumulative distributive function (CDF) of $\min(\gamma_R^{x_1}, \gamma_{UE_1}^{x_1,II}, \gamma_{UE_2}^{x_1,II}, \gamma_{UE_1}^{x_1}, \gamma_{UE_2}^{x_1})$ can be given as:

$$F_\gamma(\gamma) = 1 - \Pr\left(\frac{a_1 PX_2}{a_2 PX_2 + 1} \geq \gamma\right) \Pr\left(\frac{a_1 PX_3}{a_2 PX_3 + 1} \geq \gamma\right) \Pr\left(\frac{a_1 PX_1}{a_2 PX_1 + 1} \geq \gamma, \frac{b_1 k\eta PX_1 X_4}{b_2 k\eta PX_1 X_4 + 1} \geq \gamma, \frac{b_1 k\eta PX_1 X_5}{b_2 k\eta PX_1 X_5 + 1} \geq \gamma\right)$$

$$F_\gamma(\gamma) = 1 - \Pr\left(X_2 \geq \frac{\gamma}{P(a_1 - \gamma a_2)}\right) \Pr\left(X_3 \geq \frac{\gamma}{P(a_1 - \gamma a_2)}\right)$$

$$\times \underbrace{\Pr\left(X_1 \geq \frac{\gamma}{P(a_1 - \gamma a_2)}, X_4 \geq \frac{\gamma}{k\eta P(b_1 - b_2\gamma)X_1}, X_5 \geq \frac{\gamma}{k\eta P(b_1 - b_2\gamma)X_1}\right)}_{I_1}$$

$$F_\gamma(\gamma) = 1 - e^{-\frac{\gamma \lambda_{h_2}}{P(a_1 - \gamma a_2)}} e^{-\frac{\gamma \lambda_{h_3}}{P(a_1 - \gamma a_2)}} I_1$$

Conditioning I_1 on X_1, we get

$$F_\gamma(\gamma) = 1 - e^{-\frac{(\lambda_{h_2} + \lambda_{h_3})\gamma}{P(a_1 - \gamma a_2)}} \int_{x_1 = 0}^{\infty} \Pr\left(x_1 \geq \frac{\gamma}{P(a_1 - \gamma a_2)}, X_4 \geq \frac{\gamma}{k\eta P(b_1 - b_2\gamma)x_1}, X_5 \geq \frac{\gamma}{k\eta P(b_1 - b_2\gamma)x_1}\right) f_{X_1}(x_1) dx_1$$

$$F_\gamma(\gamma) = 1 - e^{-\frac{(\lambda_{h_2} + \lambda_{h_3})\gamma}{P(a_1 - \gamma a_2)}} \int_{x_1 = \frac{\gamma}{P(a_1 - \gamma a_2)}}^{\infty} \Pr\left(X_4 \geq \frac{\gamma}{k\eta P(b_1 - b_2\gamma)x_1}, X_5 \geq \frac{\gamma}{k\eta P(b_1 - b_2\gamma)x_1}\right) f_{X_1}(x_1) dx_1$$

$$F_\gamma(\gamma) = 1 - e^{-\frac{(\lambda_{h_2} + \lambda_{h_3})\gamma}{P(a_1 - \gamma a_2)}} \int_{x_1 = \frac{\gamma}{P(a_1 - \gamma a_2)}}^{\infty} \Pr\left(X_4 \geq \frac{\gamma}{k\eta P(b_1 - b_2\gamma)x_1}\right) \Pr\left(X_5 \geq \frac{\gamma}{k\eta P(b_1 - b_2\gamma)x_1}\right) f_{X_1}(x_1) dx_1$$

$$F_\gamma(\gamma) = 1 - e^{-\frac{(\lambda_{h_2} + \lambda_{h_3})\gamma}{P(a_1 - \gamma a_2)}} \int_{x_1 = \frac{\gamma}{P(a_1 - \gamma a_2)}}^{\infty} e^{-\frac{\lambda_{h_4}\gamma}{k\eta P(b_1 - b_2\gamma)x_1}} e^{-\frac{\lambda_{h_5}\gamma}{k\eta P(b_1 - b_2\gamma)x_1}} \lambda_{h_1} e^{-\lambda_{h_1} x_1} dx_1$$

$$F_\gamma(\gamma) = 1 - \lambda_{h_1} e^{-\frac{(\lambda_{h_2} + \lambda_{h_3})\gamma}{P(a_1 - \gamma a_2)}} \int_{x_1 = \frac{\gamma}{P(a_1 - \gamma a_2)}}^{\infty} e^{-\frac{(\lambda_{h_4} + \lambda_{h_5})\gamma}{k\eta P(b_1 - b_2\gamma)x_1} - \lambda_{h_1} x_1} dx_1$$

$$F_\gamma(\gamma) = 1 - \lambda_{h_1} e^{-\frac{(\lambda_{h_2} + \lambda_{h_3})\gamma}{P(a_1 - \gamma a_2)}} \left(\underbrace{\int_{x_1 = 0}^{\infty} e^{-\frac{(\lambda_{h_4} + \lambda_{h_5})\gamma}{k\eta P(b_1 - b_2\gamma)x_1} - \lambda_{h_1} x_1} dx_1}_{I_2} - \underbrace{\int_{x_1 = 0}^{\frac{\gamma}{P(a_1 - \gamma a_2)}} e^{-\frac{(\lambda_{h_4} + \lambda_{h_5})\gamma}{k\eta P(b_1 - b_2\gamma)x_1} - \lambda_{h_1} x_1} dx_1}_{I_3} \right)$$

The integral I_2 is in the form $\int_{x=0}^{\infty} e^{-\frac{\beta}{4x} - \gamma x} dx$ which can be solved using the formula in eq. 3.324.1 of Reference 31, as: $\frac{\beta}{\gamma} K_1(\sqrt{\beta\gamma})$, where $K_1(.)$ is a first order modified Bessel function of the second kind.

Similarly, the integral I_3 is in the form $\int_{x=0}^{a} e^{-\frac{c}{x} - bx} dx$, which can be solved in closed form[23] as: $\sum_{n=0}^{\infty} \frac{(-1)^n}{n!} b^n a^{n+1} E_{n+2}\left(\frac{c}{a}\right)$ where $E_{n+2}(.)$ is the exponential integral of order $n + 2$.

Therefore,

$$F_\gamma(\gamma) = 1 - \lambda_{h_1} e^{-\frac{(\lambda_{h_2} + \lambda_{h_3})\gamma}{P(a_1 - \gamma a_2)}} \left(2\sqrt{\frac{(\lambda_{h_4} + \lambda_{h_5})\gamma}{k\eta P \lambda_{h_1}(b_1 - \gamma b_2)}} K_1\left(2\sqrt{\frac{(\lambda_{h_4} + \lambda_{h_5})\gamma \lambda_{h_1}}{k\eta P(b_1 - \gamma b_2)}} \right) \right.$$

$$\left. - \sum_{n=0}^{\infty} \frac{(-1)^n}{n!} \lambda_{h_1}^n \left(\frac{\gamma}{P(a_1 - \gamma a_2)} \right)^{n+1} E_{n+2}\left(\frac{(\lambda_{h_4} + \lambda_{h_5})(a_1 - \gamma a_2)}{k\eta(b_1 - \gamma b_2)} \right) \right)$$

The EC in terms of CDF $F_\gamma(\gamma)$ can be written as:

$$C_{SDS-Ana}^{x_1} = \frac{(1 - \alpha)}{2 \ln 2} \int_{\gamma=0}^{\infty} \frac{1}{1 + \gamma} [1 - F_\gamma(\gamma)] d\gamma$$

Substituting $F_\gamma(\gamma)$ in the above equation, we get the final expression as in Equation (18).

This ends the proof of Theorem 1. ∎

APPENDIX B

Proof of Theorem 2. The CDF of $\min(\gamma_R^{x_2}, \gamma_{UE_2}^{x_2,II}, \gamma_{UE_2}^{x_2})$ can be given as:

$$F_\gamma(\gamma) = 1 - \Pr\left(a_2 P X_1 \geq \gamma, b_2 k \eta P X_1 X_5 \geq \gamma, a_2 P X_3 \geq \gamma\right)$$

$$F_\gamma(\gamma) = 1 - \Pr\left(X_3 \geq \frac{\gamma}{a_2 P}\right) \Pr\left(X_1 \geq \frac{\gamma}{a_2 P}, X_5 \geq \frac{\gamma}{b_2 k \eta P X_1}\right)$$

Now, conditioning $\Pr\left(X_1 \geq \frac{\gamma}{a_2 P}, X_5 \geq \frac{\gamma}{b_2 k \eta P X_1}\right)$ on X_1

$$F_\gamma(\gamma) = 1 - e^{-\frac{\lambda_{h_3} \gamma}{a_2 P}} \int_{x_1=0}^{\infty} \Pr\left(x_1 \geq \frac{\gamma}{a_2 P}, X_5 \geq \frac{\gamma}{b_2 k \eta P x_1}\right) f_{X_1}(x_1) dx_1$$

$$F_\gamma(\gamma) = 1 - e^{-\frac{\lambda_{h_3} \gamma}{a_2 P}} \int_{x_1=\frac{\gamma}{a_2 P}}^{\infty} \Pr\left(X_5 \geq \frac{\gamma}{b_2 k \eta P x_1}\right) f_{X_1}(x_1) dx_1$$

$$F_\gamma(\gamma) = 1 - \lambda_{h_1} e^{-\frac{\lambda_{h_3} \gamma}{a_2 P}} \int_{x_1=\frac{\gamma}{a_2 P}}^{\infty} e^{-\frac{\lambda_{h_5} \gamma}{b_2 k \eta P x_1} - \lambda_{h_1} x_1} dx_1$$

$$F_\gamma(\gamma) = 1 - \lambda_{h_1} e^{-\frac{\lambda_{h_3} \gamma}{a_2 P}} \left(\int_{x_1=0}^{\infty} e^{-\frac{\lambda_{h_5} \gamma}{b_2 k \eta P x_1} - \lambda_{h_1} x_1} dx_1 - \int_{x_1=0}^{\frac{\gamma}{a_2 P}} e^{-\frac{\lambda_{h_5} \gamma}{b_2 k \eta P x_1} - \lambda_{h_1} x_1} dx_1 \right)$$

$$F_\gamma(\gamma) = 1 - \lambda_{h_1} e^{-\frac{\lambda_{h_3} \gamma}{a_2 P}} \left(2\sqrt{\frac{\lambda_{h_5} \gamma}{b_2 k \eta P \lambda_{h_1}}} K_1\left(2\sqrt{\frac{\lambda_{h_1} \lambda_{h_5} \gamma}{b_2 k \eta P}}\right) - \sum_{n=0}^{\infty} \frac{(-1)^n}{n!} \lambda_{h_1}^n \left(\frac{\gamma}{a_2 P}\right)^{n+1} E_{n+2}\left(\frac{\lambda_{h_5} a_2}{b_2 k \eta}\right) \right)$$

Now, the EC in terms of CDF $F_\gamma(\gamma)$ can be written as:

$$C_{\text{SDS-Ana}}^{x_2} = \frac{1}{2 \ln 2} \int_{\gamma=0}^{\infty} \frac{1}{1+\gamma} [1 - F_\gamma(\gamma)] d\gamma$$

Substituting $F_\gamma(\gamma)$ in the above equation, we get the final expression as in Equation (20).

This ends the proof of Theorem 2. ∎

APPENDIX C

Proof of Theorem 3. The CDF of $\min(\gamma_R^{x_1}, \gamma_{UE_2}^{x_1}, \gamma_{UE_2}^{x_1,II}, \gamma_{MRC}^{x_1})$ can be given as:

$$F_\gamma(\gamma) = 1 - \Pr\left(\frac{a_1 P X_3}{a_2 P X_3 + 1} \geq \gamma\right) \Pr\left(\frac{a_1 P X_1}{a_2 P X_1 + 1} \geq \gamma, \frac{b_1 k \eta P X_1 X_5}{b_2 k \eta P X_1 X_5 + 1} \geq \gamma, \frac{a_1 P X_2}{a_2 P X_2 + 1} + \frac{b_1 k \eta P X_1 X_4}{b_2 k \eta P X_1 X_4 + 1} \geq \gamma\right)$$

$$F_\gamma(\gamma) = 1 - \Pr\left(X_3 \geq \frac{\gamma}{P(a_1 - \gamma a_2)}\right) \underbrace{\Pr\left(X_1 \geq \frac{\gamma}{P(a_1 - \gamma a_2)}, X_5 \geq \frac{\gamma}{k \eta P(b_1 - b_2 \gamma) X_1}, \frac{b_1 k \eta P X_1 X_4}{b_2 k \eta P X_1 X_4 + 1} \geq \gamma - \frac{a_1 P X_2}{a_2 P X_2 + 1}\right)}_{I_1}$$

$$F_\gamma(\gamma) = 1 - e^{-\frac{\gamma \lambda_{h_3}}{P(a_1 - \gamma a_2)}} I_1$$

Conditioning I_1 on X_1, we get

$$F_\gamma(\gamma) = 1 - e^{-\frac{\lambda_{h_3} \gamma}{P(a_1 - \gamma a_2)}} \int_{x_1=0}^{\infty} \Pr\left(x_1 \geq \frac{\gamma}{P(a_1 - \gamma a_2)}, X_5 \geq \frac{\gamma}{k \eta P(b_1 - b_2 \gamma) x_1}, \frac{b_1 k \eta P x_1 X_4}{b_2 k \eta P x_1 X_4 + 1} \geq \gamma - \frac{a_1 P X_2}{a_2 P X_2 + 1}\right) f_{X_1}(x_1) dx_1$$

$$F_\gamma(\gamma) = 1 - e^{-\frac{\lambda_{h_3} \gamma}{P(a_1 - \gamma a_2)}} \int_{x_1=\frac{\gamma}{P(a_1 - \gamma a_2)}}^{\infty} \Pr\left(X_5 \geq \frac{\gamma}{k \eta P(b_1 - b_2 \gamma) x_1}, \frac{b_1 k \eta P x_1 X_4}{b_2 k \eta P x_1 X_4 + 1} \geq \gamma - \frac{a_1 P X_2}{a_2 P X_2 + 1}\right) f_{X_1}(x_1) dx_1$$

$$F_\gamma(\gamma) = 1 - e^{-\frac{\lambda_{h_3}\gamma}{P(a_1 - \gamma a_2)}} \int_{x_1 = \frac{\gamma}{P(a_1 - \gamma a_2)}}^{\infty} e^{-\frac{\lambda_{h_5}\gamma}{k\eta P(b_1 - b_2\gamma)x_1}} \Pr\left(\frac{b_1 k\eta Px_1X_4}{b_2 k\eta Px_1X_4 + 1} \geq \gamma - \frac{a_1 PX_2}{a_2 PX_2 + 1} \right) f_{X_1}(x_1) dx_1$$

$$F_\gamma(\gamma) = 1 - e^{-\frac{\lambda_{h_3}\gamma}{P(a_1 - \gamma a_2)}} \int_{x_1 = \frac{\gamma}{P(a_1 - \gamma a_2)}}^{\infty} e^{-\frac{\lambda_{h_5}\gamma}{k\eta P(b_1 - b_2\gamma)x_1}} \underbrace{\Pr\left(\frac{b_1 k\eta Px_1X_4}{b_2 k\eta Px_1X_4 + 1} \geq \gamma - \frac{a_1 PX_2}{a_2 PX_2 + 1} \right) f_{X_1}(x_1) dx_1}_{I_2}$$

Now, conditioning I_2 on X_2, we get

$$I_2 = \int_{x_2=0}^{\infty} \Pr\left(\frac{b_1 k\eta Px_1X_4}{b_2 k\eta Px_1X_4 + 1} \geq \gamma - \frac{a_1 Px_2}{a_2 Px_2 + 1} \right) f_{X_2}(x_2) dx_2$$

Now,

$$\gamma = \frac{a_1 Px_2}{a_2 Px_2 + 1} \rightarrow x_2 = \frac{\gamma}{(a_1 - a_2\gamma)P}$$

$$I_2 = \underbrace{\int_{x_2=0}^{\frac{\gamma}{(a_1 - a_2\gamma)P}} \Pr\left(\frac{b_1 k\eta Px_1X_4}{b_2 k\eta Px_1X_4 + 1} \geq \gamma - \frac{a_1 Px_2}{a_2 Px_2 + 1} \right) f_{X_2}(x_2) dx_2}_{J_1} + \underbrace{\int_{x_2=\frac{\gamma}{(a_1 - a_2\gamma)P}}^{\infty} f_{X_2}(x_2) dx_2}_{J_2}$$

$$J_1 = \int_{x_2=0}^{\frac{\gamma}{(a_1 - a_2\gamma)P}} \Pr\left(\frac{b_1 k\eta Px_1X_4}{b_2 k\eta Px_1X_4 + 1} \geq \frac{\gamma a_2 Px_2 + \gamma - a_1 Px_2}{a_2 Px_2 + 1} \right) f_{X_2}(x_2) dx_2$$

$$J_1 = \int_{x_2=0}^{\frac{\gamma}{(a_1 - a_2\gamma)P}} \Pr\left(X_4 \geq \frac{Px_2(a_2\gamma - a_1) + \gamma}{\eta k Px_1((b_1 - \gamma b_2) + Px_2(b_1 a_2 - b_2(a_2\gamma - a_1)))} \right) \lambda_{h_2} e^{-\lambda_{h_2}x_2} dx_2$$

$$J_1 = \int_{x_2=0}^{\frac{\gamma}{(a_1 - a_2\gamma)P}} \lambda_{h_2} e^{-\frac{\lambda_{h_4}Px_2(a_2\gamma - a_1) + \gamma\lambda_{h_4}}{\eta k Px_1((b_1 - \gamma b_2) + Px_2(b_1 a_2 - b_2(a_2\gamma - a_1)))} - \lambda_{h_2}x_2} dx_2$$

Now, let $c_1 = \lambda_{h_4}P(a_2\gamma - a_1), c_2 = \lambda_{h_4}\gamma, c_3 = \eta k Px_1(b_1 - \gamma b_2), c_4 = \eta kP^2 x_1(b_1 a_2 - b_2(a_2\gamma - a_1))$

$$J_1 = \int_{x_2=0}^{\frac{\gamma}{(a_1 - a_2\gamma)P}} \lambda_{h_2} e^{-\frac{c_1 x_2 + c_2}{c_3 + c_4 x_2} - \lambda_{h_2}x_2} dx_2$$

Now, let $c_3 + c_4 x_2 = z \rightarrow dx_2 = \frac{1}{c_4}dz$

Also, when $x_2 = 0, z = c_3$ and, when $x_2 = \frac{\gamma}{(a_1 - a_2\gamma)P}, z = c_3 + c_4\frac{\gamma}{(a_1 - a_2\gamma)P} \rightarrow \hat{z}$

$$J_1 = \int_{z=c_3}^{\hat{z}} \frac{\lambda_{h_2}}{c_4} e^{-\frac{c_1\frac{(z-c_3)}{c_4} + c_2}{z} - \lambda_{h_2}\left(\frac{z - c_3}{c_4} \right)} dz$$

$$J_1 = \int_{z=c_3}^{\hat{z}} \frac{\lambda_{h_2}}{c_4} e^{-\frac{c_1}{c_4}} e^{\frac{\lambda_{h_2}c_3}{c_4}} e^{-\frac{(c_2 c_4 - c_1 c_3)}{c_4 z} - \frac{\lambda_{h_2}z}{c_4}} dz$$

Now,

$$J_2 = \int_{x_2=\frac{\gamma}{(a_1 - a_2\gamma)P}}^{\infty} f_{X_2}(x_2) dx_2 = \int_{x_2=\frac{\gamma}{(a_1 - a_2\gamma)P}}^{\infty} \lambda_{h_2} e^{-\lambda_{h_2}x_2} dx_2$$

$$J_2 = e^{-\frac{\lambda_{h_2}\gamma}{(a_1 - a_2\gamma)P}}$$

$$I_2 = J_1 + J_2$$

$$I_2 = \int_{z=c_3}^{\hat{z}} \frac{\lambda_{h_2}}{c_4} e^{-\frac{c_1}{c_4}} e^{\frac{\lambda_{h_2}c_3}{c_4}} e^{-\frac{(c_2 c_4 - c_1 c_3)}{c_4 z} - \frac{\lambda_{h_2}z}{c_4}} dz + e^{-\frac{\lambda_{h_2}\gamma}{(a_1 - a_2\gamma)P}}$$

Furthermore,

$$F_\gamma(\gamma) = 1 - e^{-\frac{\lambda_{h_3}\gamma}{P(a_1 - \gamma a_2)}} \int_{x_1 = \frac{\gamma}{P(a_1 - \gamma a_2)}}^{\infty} e^{-\frac{\lambda_{h_5}\gamma}{\eta k P(b_1 - b_2\gamma)x_1}} I_2 f_{X_1}(x_1) dx_1$$

$$F_\gamma(\gamma) = 1 - e^{-\frac{\lambda_{h_3}\gamma}{P(a_1 - \gamma a_2)}} \int_{x_1 = \frac{\gamma}{P(a_1 - \gamma a_2)}}^{\infty} e^{-\frac{\lambda_{h_5}\gamma}{\eta k P(b_1 - b_2\gamma)x_1}} \left(\int_{z=c_3}^{\hat{z}} \frac{\lambda_{h_2}}{c_4} e^{-\frac{c_1}{c_4}} e^{\frac{\lambda_{h_2}c_3}{c_4}} e^{-\frac{(c_2 c_4 - c_1 c_3)}{c_4 z} - \frac{\lambda_{h_2}z}{c_4}} dz + e^{-\frac{\lambda_{h_2}\gamma}{(a_1 - a_2\gamma)P}} \right) \lambda_{h_1} e^{-\lambda_{h_1}x_1} dx_1$$

Now, the EC in terms of CDF $F_\gamma(\gamma)$ can be written as:

$$C_{\text{MRS-Ana}}^{x_1} = \frac{(1-\alpha)}{2\ln 2} \int_{\gamma=0}^{\infty} \frac{1}{1+\gamma} [1 - F_\gamma(\gamma)] d\gamma$$

Substituting $F_\gamma(\gamma)$ in the above equation, we get the final expression as in Equation (27).
This ends the proof of Theorem 3. ∎

APPENDIX D

Proof of Theorem 4. The CDF of $\min(\gamma_R^{x_2}, \gamma_{\text{MRC}}^{x_2})$ can be given as:

$$F_\gamma(\gamma) = 1 - \Pr(a_2 P X_1 \geq \gamma, a_2 P X_3 + b_2 k\eta P X_1 X_5 \geq \gamma)$$

Conditioning on X_1, we get,

$$F_\gamma(\gamma) = 1 - \int_{x_1=0}^{\infty} \Pr\left(x_1 \geq \frac{\gamma}{a_2 P}, a_2 P X_3 + b_2 k\eta P x_1 X_5 \geq \gamma\right) f_{X_1}(x_1) dx_1$$

$$F_\gamma(\gamma) = 1 - \int_{x_1=\frac{\gamma}{a_2 P}}^{\infty} \Pr(b_2 k\eta P x_1 X_5 \geq \gamma - a_2 P X_3) f_{X_1}(x_1) dx_1$$

Again, conditioning on X_3, we get,

$$F_\gamma(\gamma) = 1 - \int_{x_1=\frac{\gamma}{a_2 P}}^{\infty} \int_{x_3=0}^{\infty} \Pr(b_2 k\eta P x_1 X_5 \geq \gamma - a_2 P x_3) f_{X_3}(x_3) dx_3 f_{X_1}(x_1) dx_1$$

Now, $\gamma = a_2 P x_3 \rightarrow x_3 = \frac{\gamma}{a_2 P}$

$$F_\gamma(\gamma) = 1 - \int_{x_1=\frac{\gamma}{a_2 P}}^{\infty} \left(\int_{x_3=0}^{\frac{\gamma}{a_2 P}} \Pr(b_2 k\eta P x_1 X_5 \geq \gamma - a_2 P x_3) f_{X_3}(x_3) dx_3 + \int_{x_3=\frac{\gamma}{a_2 P}}^{\infty} f_{X_3}(x_3) dx_3 \right) f_{X_1}(x_1) dx_1$$

$$F_\gamma(\gamma) = 1 - \int_{x_1=\frac{\gamma}{a_2 P}}^{\infty} \left(\int_{x_3=0}^{\frac{\gamma}{a_2 P}} \Pr\left(X_5 \geq \frac{\gamma - a_2 P x_3}{b_2 k\eta P x_1}\right) \lambda_{h_3} e^{-\lambda_{h_3}x_3} dx_3 + e^{-\frac{\lambda_{h_3}\gamma}{a_2 P}} \right) f_{X_1}(x_1) dx_1$$

$$F_\gamma(\gamma) = 1 - \int_{x_1=\frac{\gamma}{a_2 P}}^{\infty} \left(\int_{x_3=0}^{\frac{\gamma}{a_2 P}} \lambda_{h_3} e^{-\frac{\lambda_{h_5}\gamma - \lambda_{h_5}a_2 P x_3}{b_2 k\eta P x_1} - \lambda_{h_3}x_3} dx_3 + e^{-\frac{\lambda_{h_3}\gamma}{a_2 P}} \right) f_{X_1}(x_1) dx_1$$

$$F_\gamma(\gamma) = 1 - \int_{x_1=\frac{\gamma}{a_2 P}}^{\infty} \left(\int_{x_3=0}^{\frac{\gamma}{a_2 P}} \lambda_{h_3} e^{-\frac{\lambda_{h_5}\gamma}{b_2 k\eta P x_1}} e^{-\frac{(b_2 k\eta \lambda_{h_3}x_1 - a_2\lambda_{h_5})x_3}{b_2 k\eta x_1}} dx_3 + e^{-\frac{\lambda_{h_3}\gamma}{a_2 P}} \right) f_{X_1}(x_1) dx_1$$

$$F_\gamma(\gamma) = 1 - \int_{x_1=\frac{\gamma}{a_2 P}}^{\infty} \left(\lambda_{h_3} \frac{b_2 k\eta x_1}{b_2 k\eta \lambda_{h_3}x_1 - a_2\lambda_{h_5}} e^{-\frac{\lambda_{h_5}\gamma}{b_2 k\eta P x_1}} \left(1 - e^{-\frac{(b_2 k\eta \lambda_{h_3}x_1 - a_2\lambda_{h_5})\gamma}{b_2 k\eta x_1 a_2 P}} \right) + e^{-\frac{\lambda_{h_3}\gamma}{a_2 P}} \right) f_{X_1}(x_1) dx_1$$

$$F_\gamma(\gamma) = 1 - \int_{x_1=\frac{\gamma}{a_2 P}}^{\infty} \lambda_{h_3} \frac{b_2 k\eta x_1}{b_2 k\eta \lambda_{h_3}x_1 - a_2\lambda_{h_5}} e^{-\frac{\lambda_{h_5}\gamma}{b_2 k\eta P x_1}} \lambda_{h_1} e^{-\lambda_{h_1}x_1} dx_1$$

$$
+ \int_{x_1 = \frac{\gamma}{a_2 P}}^{\infty} \lambda_{h_3} \frac{b_2 k \eta x_1}{b_2 k \eta \lambda_{h_3} x_1 - a_2 \lambda_{h_5}} e^{-\frac{\lambda_{h_5} \gamma}{b_2 k \eta P x_1}} e^{-\frac{(b_2 k \eta \lambda_{h_3} x_1 - a_2 \lambda_{h_5}) \gamma}{b_2 k \eta x_1 a_2 P}} \lambda_{h_1} e^{-\lambda_{h_1} x_1} dx_1 - \int_{x_1 = \frac{\gamma}{a_2 P}}^{\infty} e^{-\frac{\lambda_{h_3} \gamma}{a_2 P}} \lambda_{h_1} e^{-\lambda_{h_1} x_1} dx_1
$$

$$
F_\gamma(\gamma) = 1 - \int_{x_1 = \frac{\gamma}{a_2 P}}^{\infty} \lambda_{h_1} \lambda_{h_3} \frac{b_2 k \eta x_1}{b_2 k \eta \lambda_{h_3} x_1 - a_2 \lambda_{h_5}} e^{-\frac{\lambda_{h_5} \gamma}{b_2 k \eta P x_1} - \lambda_{h_1} x_1} dx_1
$$

$$
+ \int_{x_1 = \frac{\gamma}{a_2 P}}^{\infty} \lambda_{h_3} \frac{b_2 k \eta x_1}{b_2 k \eta \lambda_{h_3} x_1 - a_2 \lambda_{h_5}} e^{-\frac{\lambda_{h_5} \gamma}{b_2 k \eta P x_1}} e^{-\frac{(b_2 k \eta \lambda_{h_3} x_1 - a_2 \lambda_{h_5}) \gamma}{b_2 k \eta x_1 a_2 P}} \lambda_{h_1} e^{-\lambda_{h_1} x_1} dx_1 - e^{-\frac{(\lambda_{h_1} + \lambda_{h_3}) \gamma}{a_2 P}}
$$

Now, the EC in terms of CDF $F_\gamma(\gamma)$ can be written as:

$$
C_{\text{MRS-Ana}}^{x_2} = \frac{(1 - \alpha)}{2 \ln 2} \int_{\gamma = 0}^{\infty} \frac{1}{1 + \gamma} [1 - F_\gamma(\gamma)] d\gamma
$$

Substituting $F_\gamma(\gamma)$ in the above equation, we get the final expression as in Equation (30).

This ends the proof of Theorem 4. ∎